

Inexpensive Electrolyte with Double-site Hydrogen Bonding and Regulated Zn²⁺
Solvation Structure for Aqueous Zn-Ion Batteries Capable of High-rate and Ultra-long
Low-Temperature Operation

Chaolin You^{1#}, Ruoyu Wu^{2#}, Xinhai Yuan¹, Lili Liu¹, Jilei Ye¹, Lijun Fu^{1,*}, Peng
Han^{2,*}, Yuping Wu^{1,*}

Experimental Section

Electrolyte configuration:

Pure aqueous electrolytes were prepared by dissolving 1 M Zn(OAc)₂ (zinc acetate, >99.9%, Aladdin) in deionized water. Hybrid electrolytes were prepared by dissolving 1 M Zn(OAc)₂ in hybrid solvents with reconstructed hydrogen bonds. The hybrid solvents were prepared by mixing formamide (FA, >99.9%, Aladdin) with deionized water. According to different proportions, the volume fraction of formamide is 10%, 30%, 50%, 60% and 70% respectively.

Synthesis of PANI:

The surface of carbon cloth was functionalized using the chronoamperometry method to optimize the hydrophile. Typical, a piece of carbon cloth with the diameter of 12 mm was held at a potential of 1.8 V for 180 s, in 1 M HClO₄ aqueous electrolyte with standard calomel electrode (SCE) and graphite foil as the reference and counter electrodes, respectively. The PANI electrodes were obtained through the copolymerization of aniline and metanilic acid on carbon cloth via a facile galvanostatic method. The 1 M HClO₄ aqueous solution containing aniline and metanilic acid with the total concentration of 0.1 M was used as the electrolyte. The SCE and graphite foil were served as the reference and counter electrodes, respectively. Electrodeposition was carried out at the current density of 0.2 mA cm⁻² for 3 h. The obtained electrodes were washed with deionized water repeatedly and dried under vacuum at 60 °C overnight. The mass loading of active material was calculated by the weight difference of the electrode before and after PANI deposition, which is around 1 mg cm⁻². The mass loading can be increased by using larger current densities for electrodeposition.

Electrolyte/Materials Characterization:

Fourier transform infrared (FTIR) and Raman spectra were collected on Nicolet IS50 spectrometer with ATR and Thermo Fisher Scientific DXR2xi with 532nm excitation, respectively. The freeze points of the different electrolytes were measured by DSC on the TA Q2000. The crystallographic structure was analyzed by X-ray diffractometer (XRD, D/MAX-IIA, Rigaku) with Cu-K α radiation ($\lambda = 0.15406$ nm) at a scanning angle (2θ) range of 10° to 90° . Scanning electron microscope (SEM) (Phenom, XL-70) images were obtained at 10 kV or 15 kV. The Energy Dispersive Spectrometer (EDS) mapping was taken at 15 kV. In-situ microscope images are obtained in real time by the combination of microscope (YM520R) and electrochemical workstation. Raman spectroscopy for the electrolyte structure was conducted on Horiba LabRAM HR Evolution microscope with a 532 nm excitation laser.

Fabrication of symmetric/asymmetric and Zn||PANI full battery:

For Zn||Zn symmetric battery, two pieces of polished Zn foils with a thickness of 100 μm ($\Phi 15$ mm) were used as two electrodes for symmetric cell. Different electrolytes were added into the CR2025-type coin cell with a piece of glass fiber (GF/A, Whatman) as a separator. For Zn||Cu asymmetric battery, the same assembly process, the only difference being the replacement of one side of the Zn foil with a Cu foil (32 μm , $\Phi 15$ mm). The Zn||PANI full cells were fabricated with Zn foils and PANI with glass fiber (GF/A Whatman) as the separator in CR2025 coin cells.

Electrochemical Characterization:

The performances of Zn||Zn symmetric batteries Zn||Cu asymmetric batteries, and Zn||PANI full batteries were collected by a LAND battery test system (CTA2001A, Wuhan Land Electronic Co. Ltd.). The linear scan voltammetry (LSV), Chronoamperograms (CAs) are carried out utilizing an electrochemical workstation (CHI 660E Chenhua, Shanghai). A Low temperature test chamber (Nanjing MJS Energy Technology Co. Ltd.) was used to provide the constant temperature environment for electrochemical tests. All the tests were carried out after samples being maintained at the specified temperature for 3 hours. The ionic conductivity of the electrolytes was measured at different temperatures through EIS with cells consisted of

two parallel Pt-plate electrodes (1 cm × 1 cm). The applied frequency range was from 1000 Hz to 0.1 Hz with an AC amplitude of 5 mV. The electrolyte resistance was acquired from the intercept of Nyquist plot and the ionic conductivity was calculated according to the following equation:

$$\sigma = G \frac{L}{A} = \frac{L}{R_s A}$$

Where σ (S cm⁻¹) is the per unit conductivity, G (S) is conductance, R_s is the electrolyte resistance, L (cm) is interval distance (1 cm) between the two Pt-plate electrodes, A (1 cm²) is electrode area.

Density functional theory calculations:

Ab initio density functional theory (DFT) calculations at the level of B3LYP with 6-311G(d,p) basis set were carried out to study the binding energy and the solvation energy of Zn(OAc)₂-FA electrolyte system using Gaussian 16 code package. The implicit universal water solvation model based on the idea of solute electron density (SMD) was applied in the solvation energy calculation. To accurately describe the weak interaction between ions and molecules, DFT-D3 correction was used to conduct the total energy of the optimized structures. The binding energy $E_{binding}$ of a configuration AB was calculated via the relation,

$$E_{binding} = E(AB) - E(A) - E(B) \quad (1)$$

where, $E(A)$, $E(B)$, and $E(AB)$ denote the total energy of ion (molecule) A , B and their configuration, respectively. The solvation energy of solvation structure $[Zn(H_2O)_m(CH_3NO)_n(CH_3COO)_k]^{(2-k)+}$ was calculated as,

$$\begin{aligned} \Delta E_{solvation} &= E(Zn^{2+} + mH_2O + nCH_3NO + kCH_3COO^-) - E(Zn^{2+}) - mE(H_2O) - \\ & nE(CH_3NO) - kE(CH_3COO^-) \end{aligned} \quad (2)$$

where m , n , and k denote the coordination numbers of the solvation structure.

To investigate the absorption energy E_{abs} of H₂O and FA molecules on Zn (002) surface at hollow, top, and bridge sites, we perform ab initio DFT calculations to calculate the

total energy of the Zn (002) surface $E(\text{surface})$, the adsorbent molecule $E(\text{adsorbent})$ and the system of Zn surface with the adsorbent molecule $E(\text{surface} + \text{adsorbent})$. The adsorption energy is then obtained by the following equation,

$$E_{\text{abs}} = E(\text{surface} + \text{adsorbent}) - E(\text{surface}) - E(\text{adsorbent}).$$

The ab initio calculations for the adsorption energy were performed using the CP2K code package¹ based on the framework of local density approximation functional and a hybrid Gaussian and plane-wave scheme. Molecular orbitals of the valence electrons are expanded into the DZVP-GTH-PADE basis sets² while the plane waves were expanded with a cutoff energy of 400 Rydberg. The Goedecker-Teter-Hutter (GTH) pseudopotentials were used to describe the atomic core electrons³. In the DFT calculation, dispersion correction was applied within the framework of the DFT-D3 method⁴. A 5×5 supercell of Zn (002) surface with five atomic layers was constructed to model the Zn surface, while H₂O and FA molecules attached at the hollow, top, and bridge sites were employed to mimic the adsorbent molecules. To avoid the charge interaction between neighboring images under the periodic boundary conditions, a vacuum of 30 Å in the z direction was used.

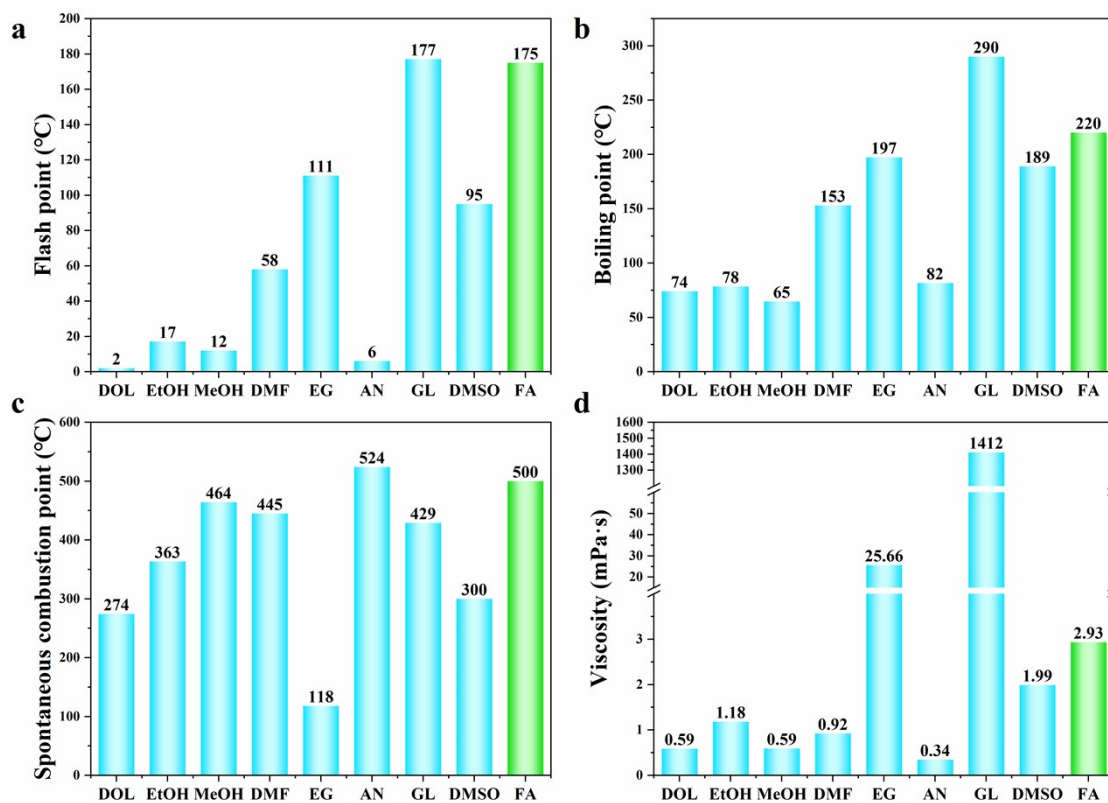


Figure S1 Comparison of the physicochemical properties for different organic solutions: Flash point (a), Boiling point (b), Spontaneous combustion point (c) and Viscosity (d).

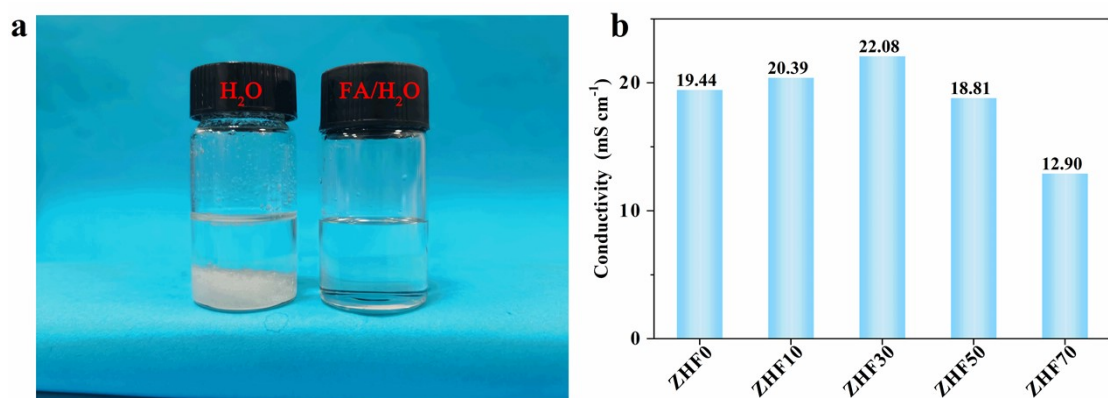


Figure S2 a) Dissolution status of salt in pure aqueous solvents and FA- H_2O mixed solvents. b) Ionic conductivities of different electrolytes with different volume ratio between H_2O and FA (the electrolytes are denoted as ZHF x , with x representing a volume fraction of $x\%$ for FA).

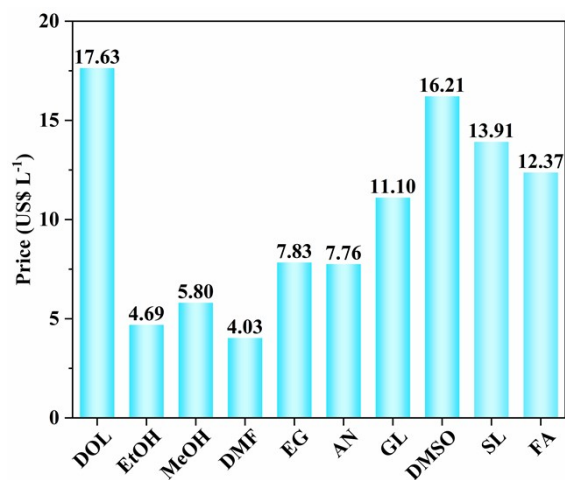


Figure S3 Price of some commonly reported solvents and FA. Note: Price information on these Zn salts and solvents was mainly taken from <https://www.aladdin-e.com> (Aladdin, one of the major reagent suppliers in China) on 25 May, 2023.

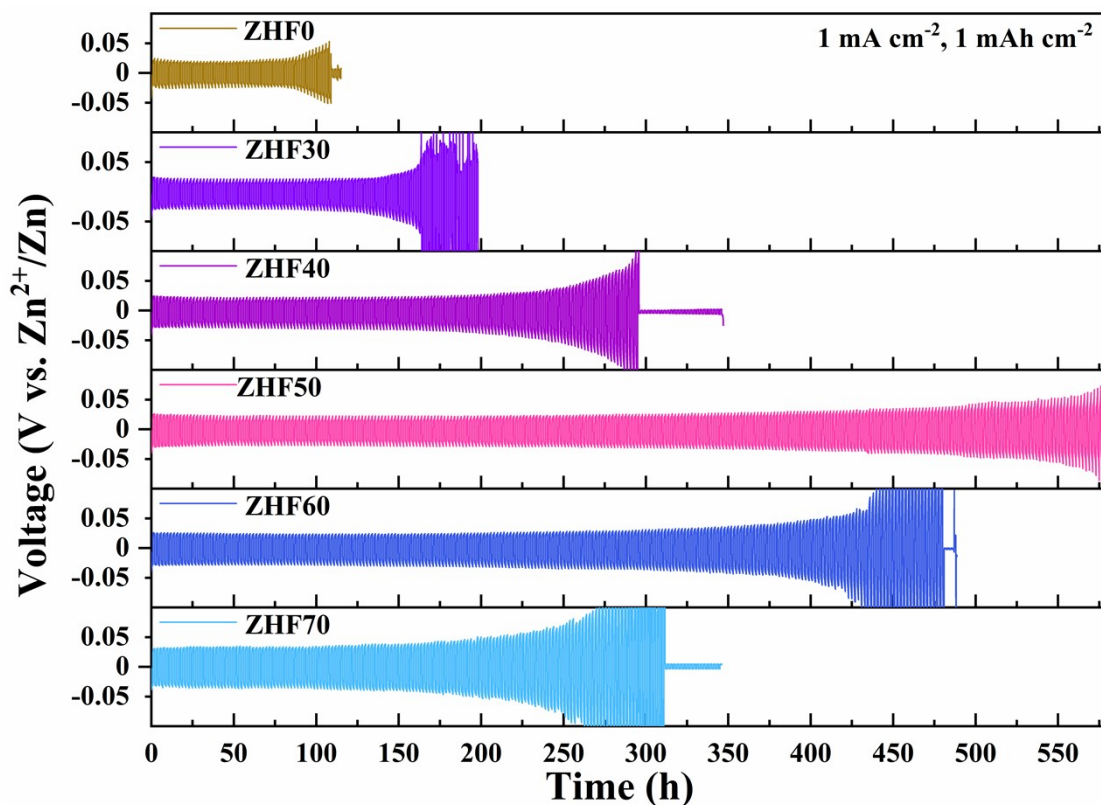


Figure S4 The voltage profiles of Zn||Zn symmetrical batteries cycling at 1 mA cm⁻² under 25 °C. The symmetric cell with ZHF50 offers the longest life, and further increasing or decreasing the FA ratio leads to a shorter life for the symmetric cell.

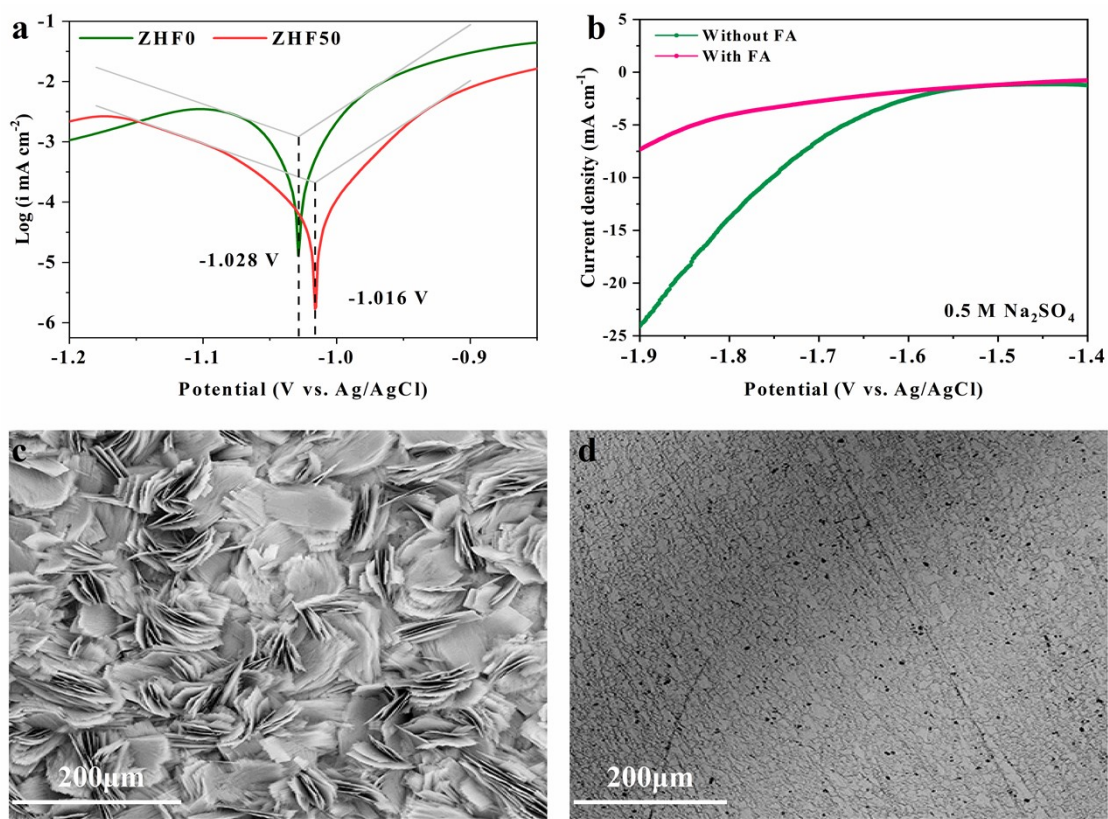


Figure S5 a) Tafel plots of Zn anode in different electrolytes. b) Linear scanning voltammetry curves in 0.5 M aqueous Na_2SO_4 electrolyte with/without FA—working electrode: Zn foil, counter electrode: Pt, and reference electrode: Ag/AgCl (saturated KCl). SEM images of the Zn foil immersed in the (c) ZHF0 and (d) ZHF50 electrolyte after 15 days.

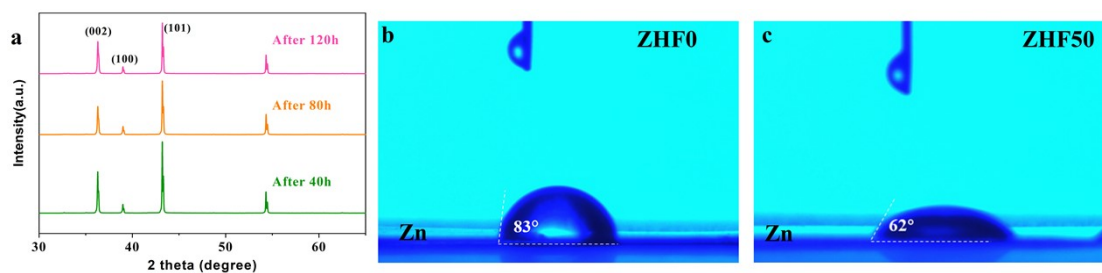


Figure S6 a) XRD patterns of Zn metal with ZHF0 after different cycle time at 1.0 mA cm^{-2} in a symmetrical Zn battery. Wetting angles of (b) H_2O and (c) FA droplet on Zn foil.

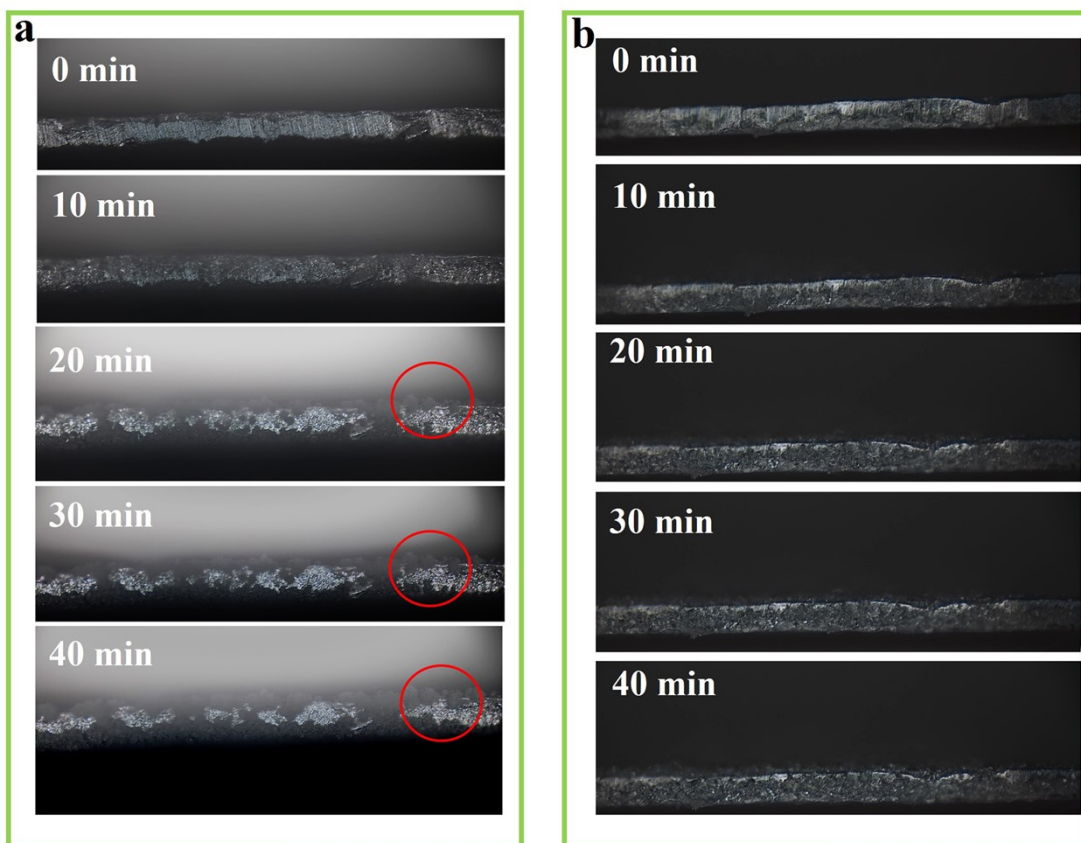


Figure S7 Cross-sectional Zn deposition morphology with different electrolytes (a) ZHF0 and (b) ZHF50 in a symmetrical Zn battery at a current density of 5 mA cm^{-2} using an in situ optical microscope.

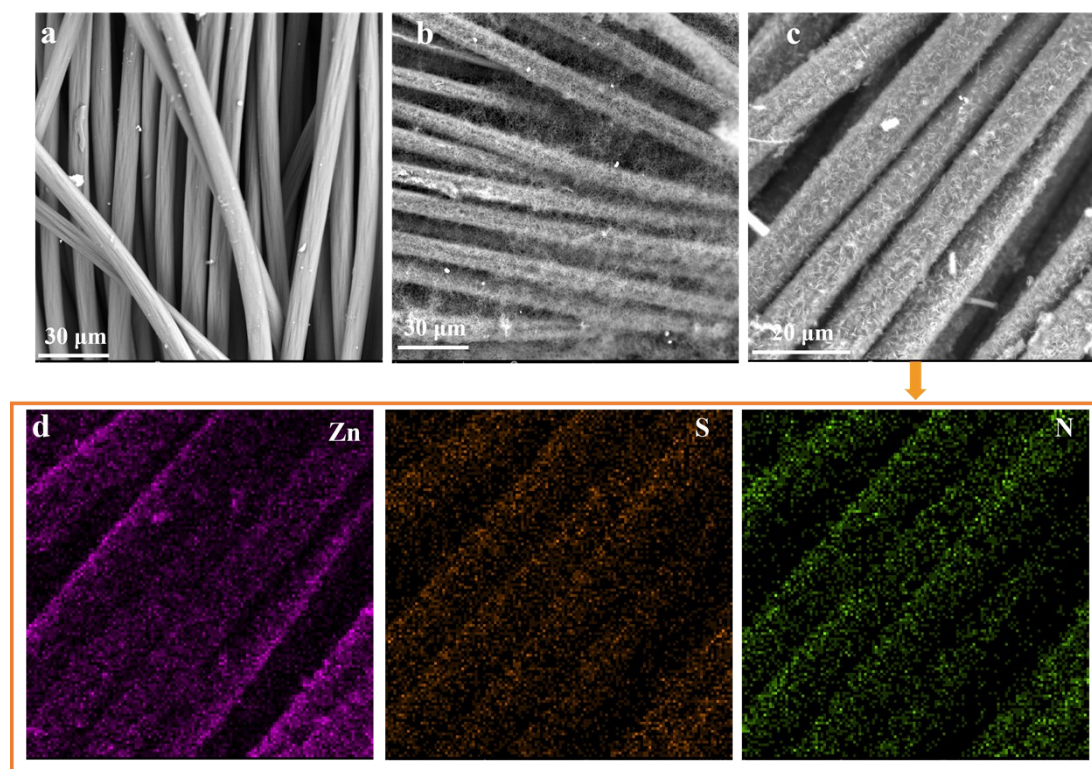


Figure S8 SEM images of a) Carbon Cloth, b) the PANI electrodeposited on carbon cloth, and c) PANI after discharge and d) the corresponding elemental distribution.

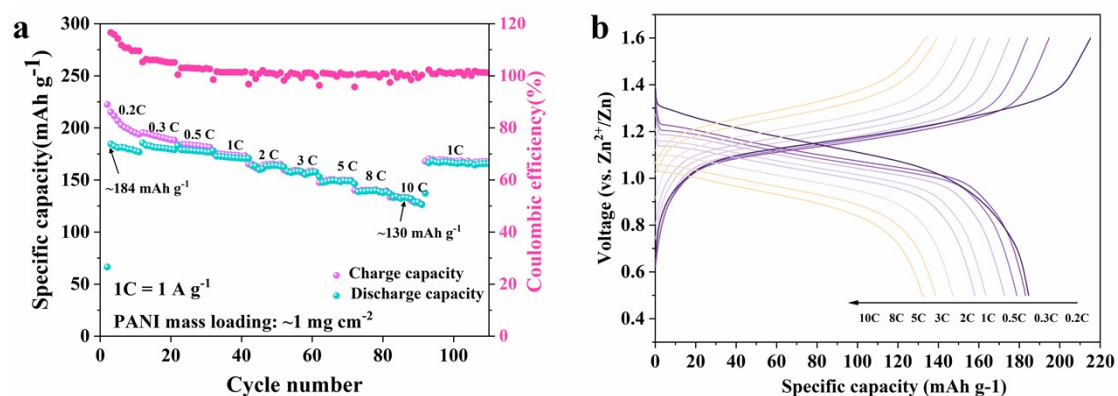


Figure S9 Electrochemical performance of the Zn||PANI batteries with ZHF50 under 25°C. a) Rate performance and b) Charge/discharge curves.

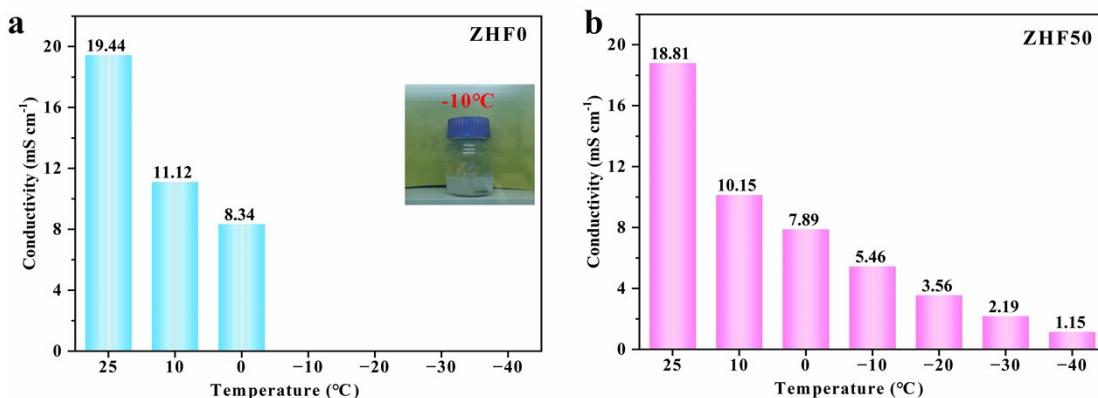


Figure S10 The ionic conductivity under different temperature for (a) ZHF0 electrolyte (The inset shows optical photograph of ZHF0 electrolyte at -10°C .) and (b) ZHF50 electrolyte.

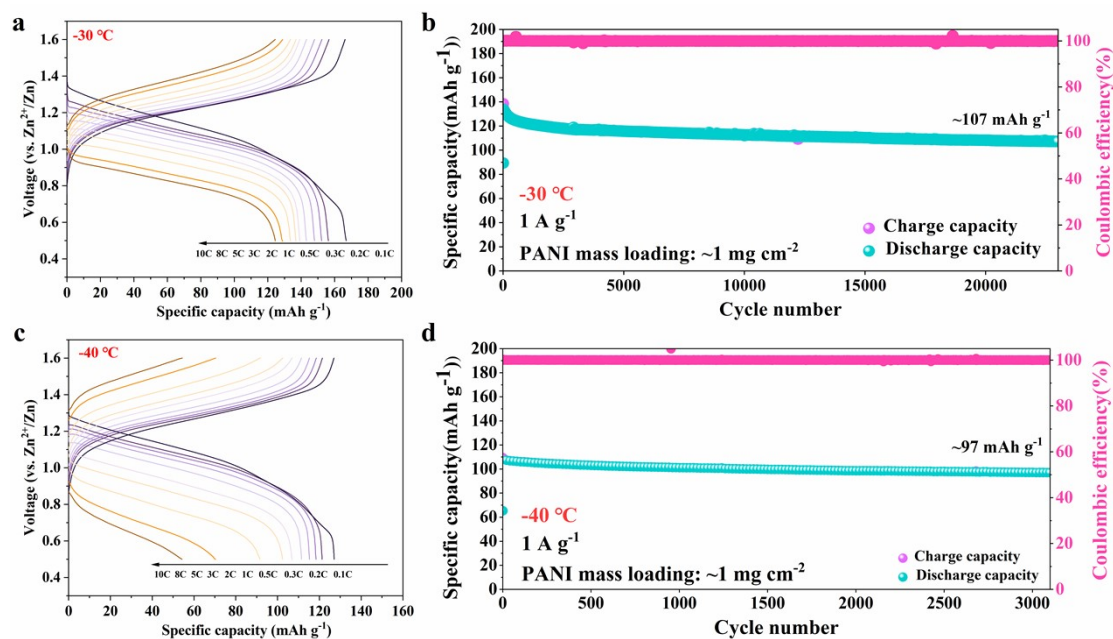


Figure S11 Electrochemical performance of the Zn||PANI batteries with ZHF50 at low temperature. Charge/discharge curves a) under -30°C and c) under -40°C . Long-term cycling at 1 A g^{-1} b) under -30°C and d) under -40°C .

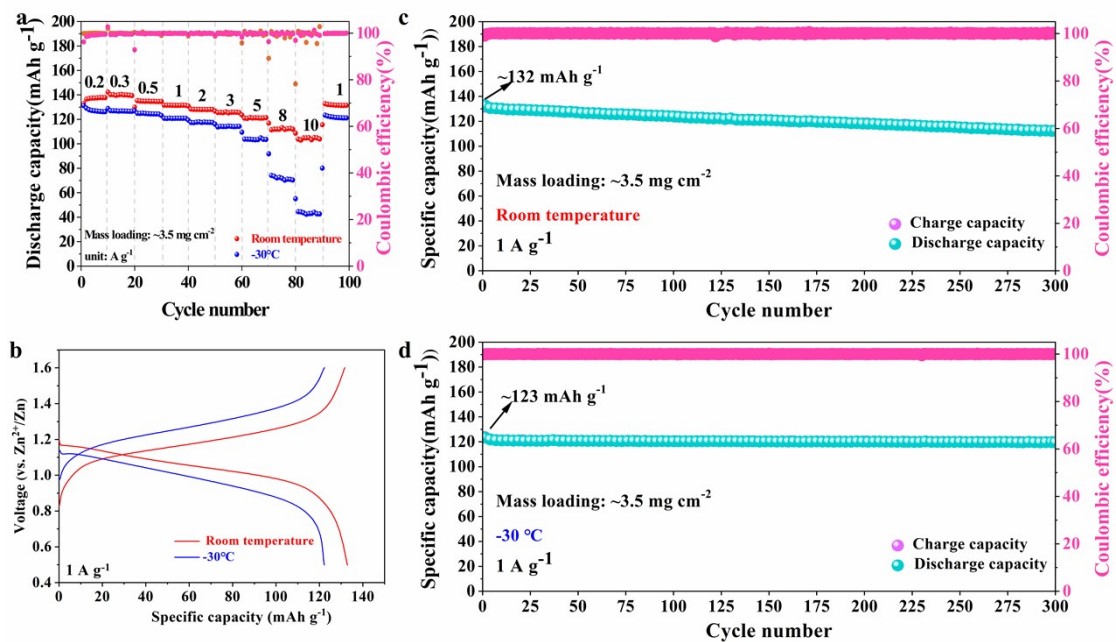


Figure S12 Electrochemistry of the Zn||PANI batteries with $\sim 3.5 \text{ mg cm}^{-2}$ PANI mass loading. a) Rate performance and b) Charge/discharge curves at different temperature. Long-term cycling at 1 A g^{-1} c) under room temperature and d) under -30°C .

Table S1 Performance of low-temperature Zn symmetrical cells of our work and the reported works.

Electrolyte	Temp. (°C)	Current density (mA cm ⁻²)	Cumulative capacity (mAh cm ⁻²)	Cycling lifetime (h)	Reference
4 M Zn(BF ₄) ₂	-30	0.5	375	1500	5
7.5 m ZnCl ₂	-70	0.2	50	500	6
6.0 M KOH+0.20 M Zn(OAc) ₂	-10	10	70	28	7
	-20	5	150	30	
3 M Zn(CF ₃ SO ₃) ₂	-30	0.2	40	400	8
1M Zn(Tof) ₂ (72 vol% AN+28 vol% H ₂ O)	-40	5	1250	>500	9
	-50	2	50	~50	
2 M ZnSO ₄ (40 vol% EG+60 vol% H ₂ O)	-20	2	80	80	10
2 M ZnSO ₄ (20 vol% DMSO +80 vol% H ₂ O)	-20	0.5	300	1200	11
Zn(ClO ₄) ₂ ·6H ₂ O·6Sulfolane	-30	0.2	20	200	12
CMCS/PAM hydrogel (polysaccharides carboxymethyl chitosan/polyacrylamide + Zn(ClO ₄) ₂)	-30	1	500	1000	13
PAM ZS/GL/AN hydrogel (polyacrylamide/ZnSO ₄ / glycerol /acetonitrile)	-20	0.2	50	500	14
GG/SA/EG (guar-gum/sodium-alginate/ethylene-glycol) hydrogel-based electrolyte	-20	0.2	20	200	15
1 M Zn(OAc)₂ (50 vol% FA+50 vol% H₂O)	-30	1	2600	5200	This work
	-40	0.5	192	770	

Table S2 The rate and cycling performance of the batteries with ZHF50 electrolyte compared with current reported Zn-PANI batteries.

Electrolyte	Cathode	Temp. (°C)	Specific capacity/Rate performance	Cycle performance	Reference
1 M Zn(OAc) ₂ (50 vol% FA+50 vol% H ₂ O)	PANI	-30 °C	124.8 mAh g ⁻¹ at 10 A g ⁻¹	121 mAh g ⁻¹ at 5 A g ⁻¹ after 5500 cycles	This work
		-40 °C	54.5 mAh g ⁻¹ at 10 A g ⁻¹	80 mAh g ⁻¹ at 5 A g ⁻¹ after 6500 cycles	
CSAM-C gel	PANI	-30 °C	76 mAh g ⁻¹ at 5 A g ⁻¹	70 mAh g ⁻¹ at 5 A g ⁻¹ after 2500 cycles	13
Methanol-50%	PANI	-10 °C	~117 mAh g ⁻¹ at 5 A g ⁻¹	~105 mAh g ⁻¹ at 5 A g ⁻¹ after 2000 cycles	16
CPAM gel	PANI	-20 °C	~137 mAh g ⁻¹ at 0.2 A g ⁻¹	~120 mAh g ⁻¹ at 0.2 A g ⁻¹ after 600 cycles	17
Zn(ClO ₄) ₂ ·6H ₂ O·6Sulfolane	PANI	-30 °C	~80 mAh g ⁻¹ at 0.3 A g ⁻¹	73 mAh g ⁻¹ at 0.3 A g ⁻¹ after 500 cycles	12
PAMPS/PAAm gel	PANI	-30 °C	59.7 mAh g ⁻¹ at 1 A g ⁻¹	~97 mAh g ⁻¹ at 0.2 A g ⁻¹ after 1500 cycles	18
DMF-30%	PANI	-40 °C	65.8 mAh g ⁻¹ at 0.2 A g ⁻¹	NA	19
3 M Zn(OTf) ₂	PANI	-40 °C	~55 mAh g ⁻¹ at 0.2 A g ⁻¹	101.4 mAh g ⁻¹ at 0.5 A g ⁻¹ after 5000 cycles	20
ZnCl ₂ -LiCl BC gel	PANI	-30 °C	~100 mAh g ⁻¹ at 5 A g ⁻¹	132.4 mAh g ⁻¹ at 0.5 A g ⁻¹ after 1000 cycles	21
PVA-EG gel	PANI	-20 °C	52 mAh g ⁻¹ at 2 A g ⁻¹	~73 mAh g ⁻¹ at 1 A g ⁻¹ after 150 cycles	22

DMF: N, N-dimethylformamide

BC: bacterial cellulose

Reference:

1. T. D. Kuhne, M. Iannuzzi, M. Del Ben, V. V. Rybkin, P. Seewald, F. Stein, T. Laino, R. Z. Khaliullin, O. Schutt, F. Schiffmann, D. Golze, J. Wilhelm, S. Chulkov, M. H. Bani-Hashemian, V. Weber, U. Borstnik, M. Taillefumier, A. S. Jakobovits, A. Lazzaro, H. Pabst, T. Muller, R. Schade, M. Guidon, S. Andermatt, N. Holmberg, G. K. Schenter, A. Hehn, A. Bussy, F. Belleflamme, G. Tabacchi, A. Gloss, M. Lass, I. Bethune, C. J. Mundy, C. Plessl, M. Watkins, J. VandeVondele, M. Krack and J. Hutter, *J. Chem. Phys.*, 2020, **152**, 194103.
2. J. VandeVondele and J. Hutter, *J. Chem. Phys.*, 2007, **127**, 114105.

3. S. G. C. Hartwigsen, J. Hutter, *Phys. Rev. B*, 1998, **58**, 3641.
4. S. Grimme, J. Antony, S. Ehrlich and H. Krieg, *J. Chem. Phys.*, 2010, **132**, 154104.
5. T. Sun, X. Yuan, K. Wang, S. Zheng, J. Shi, Q. Zhang, W. Cai, J. Liang and Z. Tao, *J. Mater. Chem. A*, 2021, **9**, 7042-7047.
6. Q. Zhang, Y. Ma, Y. Lu, L. Li, F. Wan, K. Zhang and J. Chen, *Nat. Commun.*, 2020, **11**, 4463.
7. C. X. Zhao, J. N. Liu, N. Yao, J. Wang, D. Ren, X. Chen, B. Q. Li and Q. Zhang, *Angew. Chem. Int. Ed. Engl.*, 2021, **60**, 15281-15285.
8. Q. Zhang, K. Xia, Y. Ma, Y. Lu, L. Li, J. Liang, S. Chou and J. Chen, *ACS Energy Letters*, 2021, **6**, 2704-2712.
9. J. Wang, Q. Zhu, F. Li, J. Chen, H. Yuan, Y. Li, P. Hu, M. S. Kurbanov and H. Wang, *Chem. Eng. J.*, 2022, **433**, 134589.
10. N. Chang, T. Li, R. Li, S. Wang, Y. Yin, H. Zhang and X. Li, *Energy Environ. Sci.*, 2020, **13**, 3527-3535.
11. D. Feng, F. Cao, L. Hou, T. Li, Y. Jiao and P. Wu, *Small*, 2021, **17**, e2103195.
12. X. Lin, G. Zhou, M. J. Robson, J. Yu, S. C. T. Kwok and F. Ciucci, *Adv. Funct. Mater.*, 2021, **32**, 2109322.
13. S. Huang, L. Hou, T. Li, Y. Jiao and P. Wu, *Adv. Mater.*, 2022, **34**, e2110140.
14. T. Wei, Y. Ren, Z. Li, X. Zhang, D. Ji and L. Hu, *Chem. Eng. J.*, 2022, **434**, 134646.
15. J. Wang, Y. Huang, B. Liu, Z. Li, J. Zhang, G. Yang, P. Hiralal, S. Jin and H. Zhou, *Energy Storage Mater.*, 2021, **41**, 599-605.
16. J. Hao, L. Yuan, C. Ye, D. Chao, K. Davey, Z. Guo and S. Z. Qiao, *Angew. Chem. Int. Ed. Engl.*, 2021, **60**, 7366-7375.
17. X. Jin, L. Song, C. Dai, H. Ma, Y. Xiao, X. Zhang, Y. Han, X. Li, J. Zhang, Y. Zhao, Z. Zhang, L. Duan and L. Qu, *Energy Storage Mater.*, 2022, **44**, 517-526.
18. X. Li, H. Wang, X. Sun, J. Li and Y.-N. Liu, *ACS Appl. Energy Mater.*, 2021, **4**, 12718-12727.
19. Y. Ma, Q. Zhang, L. Liu, Y. Li, H. Li, Z. Yan and J. Chen, *Natl. Sci. Rev.*, 2022, **9**, nwac051.
20. D. Wang, D. Lv, H. Peng, N. Wang, H. Liu, J. Yang and Y. Qian, *Nano Lett.*, 2022, **22**, 1750-1758.
21. C. Yan, Y. Wang, X. Deng and Y. Xu, *Nanomicro Lett*, 2022, **14**, 98.
22. Z. Cong, W. Guo, P. Zhang, W. Sha, Z. Guo, C. Chang, F. Xu, X. Gang, W. Hu and X. Pu, *ACS Appl. Mater. Interfaces*, 2021, **13**, 17608-17617.